Proceedings of the 5th WSEAS Int. Conf. on Power Systems and Electromagnetic Compatibility, Corfu, Greece, August 23-25, 2005 (pp149-155)

THE LAPLACE TRANSFORM BASED FREQUENCY ANALYSIS IN FOUR-SWITCH SPACE-VECTOR MODULATED VSI

JIRI KLIMA
Department of Electrical Engineering and Automation, Technical Faculty of CZU in Prague, 16521, Prague6-Suchdol, Czech Republic,
Tel.:+420224343203,Fax.:+420224381828

Abstract .The paper presents closed-form expressions for the harmonic components of the space-vector modulated waveforms for improved electric drive reliability. The analysis is based on space-vector decomposition technique for finding the symmetrical vector sequences. From the Laplace transform of the symmetrical voltage vectors we can derive relations for the harmonic spectrum. The harmonic spectrum are compared and verified with the measured results. As shown, there is an excellent agreement between the analytically calculated waveforms and the experimentally

Key-Words: Fourier analysis, Harmonic spectrum, Modulation, Voltage Source Inverters

1 Introduction

Modern AC motor drive systems are predominantly based on three-phase voltage source inverters (VSI). But VSI fed induction motor drives are prone to shoot through and other inverter faults that cause the drive system to shut down .A three phase inverter can develop various faults of which open base drive and shoot through are most common. These faults have been analyzed in detail in [1],[2].When AC drives are used in critical manufacturing processes possible operation interruption may lead to the shutdown of the whole process.. So improved reliability and fault tolerant operation of these drives is important.

Most commonly, many of the power converter failures are caused by the loss of conduction of one inverter leg. In general, when one of these faults does occur, the isolation of the fault is preferable since it keeps the drive partially operative.

Several remedial operating strategies applied to the three-phase induction motor drives to improve their reliability can be found in the literature. Most of them are based on extra connections between the motor and the voltage source inverter. In [3] two-phase operation mode is proposed , by connecting the motor stator windings neutral point to the DC supply. Additionally, a 60^0 phase shifted current reference was also introduced to minimize the electromagnetic torque ripple component. An altermative approach to minimize the low-frequency pulsating torque was proposed in [4] based on the injection of odd voltage harmonic at appropriate phase angles. In [5] is proposed a topology based on connection of the motor stator windings neutral to a forth additional inverter leg.

But in these strategies as the neutral point of winding is connected, some additional problems like the flowing of zero-sequence currents into the there-phase induction motor and increasing both phase currents and torque pulsation.

The paper presents an analytical model for frequency-domain analysis and comparison of space-vector modulated inverter fed induction motor drive in a normal (B6) and four-switch inverters (B4). To verify the proposed mathematical model, a prototype of the inverter has been built. A very close agreement has been established between the measured and analytical harmonic spectra. All the analytical results were visualized from the derived equations by the programme MATCAD [12].

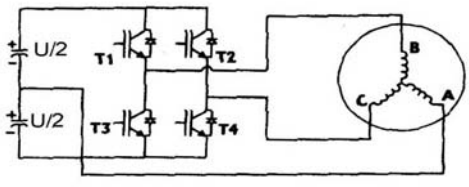

Fig.-1. VSI under consideration

2 Proposed Space-Vector Modulation

The B4 inverter employs only four switches and four diodes to generate phase voltages.

The four switch inverter cannot produce any null switching state like those in the six switch inverter and so in order to regulate magnitude of the voltage vector $\mathbf{V}_{AV}$, another mechanism is needed.

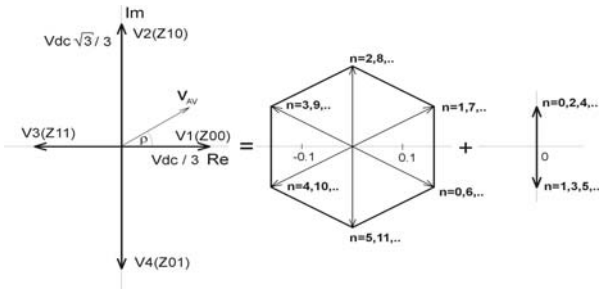

Fig.-2. Four voltage vectors (left) and their symmetrical components (right)

As there are four switching states we can find four possible voltage vectors **V**1, **V2, V3** and **V**4 in complex αβ plane as shown in Fig.2 (left). These vectors are π/2 away from each other. Also they do not have the same amplitude as in the classical B6 connection. Vectors laying in the real axis have amplitude of $V_{dc}/3$, whereas the vectors lying in the imaginary axis have amplitude of $\sqrt{3}V_{dc}/3$. The vectors in Fig.2 have the following denotation:

$$\mathbf{V}_1\ (Z00),\ \mathbf{V2}\ (Z10),\ \mathbf{V3}\ (Z11),\ \mathbf{V4}\ (Z01) \qquad (1)$$

Where (Z,S_B,S_C) in (1), denotes the inverter switching states, in which S_i=1 (i=B.C) if the upper leg switch is on and S_i=0 if the upper leg switch is off. Z means zero pole voltage v_A= 0 .

If we use six voltage vectors per fundamental period:

$$\mathbf{V}_1\ (Z00),\ \mathbf{V}_1\ (Z00),\ \mathbf{V}_2\ (Z10),\ \mathbf{V}_3\ (Z11),\mathbf{V}_3\ (Z11),\ \mathbf{V}_4\ (Z01), \qquad (2)$$

We get for the sector period:

$$T = \frac{T_1}{6}$$

where T_1 is a period of output voltage .

It means that the sector period has the same value as in the B6 inverter.

The vector sequence (2) is unsymmetrical and using Discrete Fourier Transform (DFT) it may be expressed in the symmetrical form as follows:

$$V(n) = \frac{1}{N}\sum_{m=0}^{N-1} V(m) \sum_{i=0}^{N-1} e^{ji(n-m)\frac{2\pi}{N}} \qquad (3)$$

Where N is number of the used vectors. Substituting (2) into (3) we get for the symmetrical components:

$$V(n) = \frac{V_{dc}}{3}\frac{2}{\sqrt{3}}e^{-j\pi/6}e^{j\pi\frac{n}{3}} + \frac{V_{dc}}{3}\frac{1}{\sqrt{3}}e^{j\pi/2}e^{j\pi n} = V_1(n) + V_3(n) \qquad (4)$$

As can be seen from (4) the unsymmetrical vector sequence (2) can be decomposed into two symmetrical ones. The first sequence has symmetry π/3 as in the conventional B6 inverter, but its amplitude is lowered by 1/√3 times and the phase is rotated by (-π/6) as compared with the conventional B6 inverter**.**

The second symmetrical sequence is laying in the imaginary axis and it has amplitude lowered by two times compared with the first sequence. Because of its period, this sequence will form the third order voltage harmonics in the output cycle period. This indicates that in the phase A (commonly in the phase connected with the midpoint of DC-link) can not originate any voltage source given by this alternating sequence. In the both remaining phases the voltage given by an alternating sequence must have the opposite sign and the same magnitudes to cancel each other out. The both symmetrical sequence components are also shown in Fig.2 (right).

The modulation strategy which is proposed for the B4 inverter has the same symmetry as for the B6 inverter and is simple without significant increase in switching frequency The proposed modulation strategy is realized by planning the switching patterns between four active voltage vectors within a sampling period $\Delta T = T/N_1$ aims :

a) Utilizing the first voltage vector sequence term $\mathbf{V}_1(n)$ in (4). As in the classical space vector modulation four consecutive voltage vectors in a sampling period are used to generate the average output voltage matching with the reference voltage $\mathbf{V}_{AV}$.
b) Minimizing the second voltage vector sequence term $\mathbf{V}_3(n)$ in (4). For minimization, the average voltage from

the $\mathbf{V}_3(n)$ within a sampling period should be zero.

If we have command vector $\mathbf{V}_{AV}$ placed in the complex αβ plane as shown in Fig.2, the following two equations should be satisfied for conditions a) and b) in the proposed SVM, respectively:

$$\frac{2}{3\sqrt{3}}V_{dc}.\Delta T_1.e^{-j\pi/6}+\frac{2}{3\sqrt{3}}V_{dc}.\Delta T_2.e^{j\pi/6}+\frac{2}{3\sqrt{3}}V_{dc}.\Delta T_3.e^{j\pi/2}+\frac{2}{3\sqrt{3}}V_{dc}.\Delta T_4.e^{j5\pi/6}=V_{AV}.\Delta T.e^{j\rho} \quad (5)$$

$$\Delta T_1+\Delta T_3=\Delta T_2+\Delta T_4 \quad (6)$$

In addition the time portions allocated to each vector are given by constrain:

$$\Delta T_1+\Delta T_2+\Delta T_3+\Delta T_4=\Delta T \quad (7)$$

Where $\Delta T_1, \Delta T_2, \Delta T_3$, and ΔT_4 are the respective vector time intervals, ρ is a polar angle of the reference voltage $\mathbf{V}_{AV}$ to the real axis given by (8):

g is a modulation factor :

$$g=\frac{2\sqrt{3}V_{AV}}{V_{dc}} \quad (8)$$

Solving (5), (6) and (7) we get for the switching time intervals (in per units):

$$\Delta\varepsilon_1=\frac{\Delta T_1}{T}=\frac{1}{2N_1}-\frac{g}{2N_1}\sin\rho$$

$$\Delta\varepsilon_2=\frac{\Delta T_2}{T}=\frac{g}{2N_1}\sin(\rho+\pi/3) \quad (9)$$

$$\Delta\varepsilon_3=\frac{\Delta T_3}{T}=\frac{g}{2N_1}\sin\rho$$

$$\Delta\varepsilon_4=\frac{\Delta T_4}{T}=\frac{1}{2N_1}-\frac{g}{2N_1}\sin(\rho+\pi/3)$$

Similary, as for the B6 inverter we can express the symmetrical sequence components in the time and angle dependencies as follow:

$$\mathbf{V}(n,\varepsilon)=\mathbf{V}_1(n,\varepsilon)+\mathbf{V}_3(n,\varepsilon)$$

$$=\sum_{k=1}^{M}\frac{V_{dc}}{3}\left(\frac{2}{\sqrt{3}}.e^{j(n-1/2)\pi/3}.f(\varepsilon,k).e^{j\pi\alpha(k)/3}\right)+\sum_{k=1}^{M}\frac{V_{dc}}{3}\left(\frac{1}{\sqrt{3}}.e^{j(n+1/2)\pi}.f(\varepsilon,k).e^{j\pi\alpha(k)}\right) \quad (10)$$

where time is expressed in per unit as follows:

$$t=(n+\varepsilon)T \quad (11)$$

n in (11) is number of sector, and $0\le\varepsilon\le1$

M is number of the vectors that are used within sector T. In the proposed modulation strategy four adjacent voltage vectors are utilized. The directions of these four vectors are given by the corresponding angles: $\frac{\pi}{3}\alpha(k)$ and $\pi\alpha(k)$, respectively, where k=1, 2, 3, and 4.

For four adjacent vectors we use the following values of the coefficients α (k): $\alpha(1)=0$, $\alpha(2)=1$. $\alpha(3)=2$ and $\alpha(4)=3$

The switching function f (ε, k) describing switching patter is defined similarly as for the B6 inverter:

$f(\varepsilon,k)=1$ if $\varepsilon_{kB}\ge\varepsilon\ge\varepsilon_{kA}$ (12)

$f(\varepsilon,k)=0$ else

where ε_{kA}, ε_{kB} is again the start point setting time, and the end point setting time, respectively, of k-the voltage vector. The per unit switching time intervals are:

$\Delta\varepsilon_k=\varepsilon_{kB}-\varepsilon_{kA}$, and they are defined by (9).

3 Frequency-domain model

Base on relation between the Laplace and modified Z-transform [9] we can express the Laplace transform of (10) as follows:

$\mathbf{V}(p)=\mathbf{V}_1(p)+\mathbf{V}_3(p)=$

$$\frac{1}{p}\frac{2.V_{dc}}{3\sqrt{3}}\left[\frac{e^{pT}.e^{-j\pi/6}}{e^{pT}-e^{j\pi/3}}\sum_{k=1}^{M}e^{j\pi\alpha(k)/3}(e^{-pT\varepsilon kA}-e^{-pT\varepsilon kB})\right]+\frac{1}{p}\frac{V_{dc}}{3\sqrt{3}}\left[\frac{e^{pT}.e^{j\pi/2}}{e^{pT}-e^{j\pi}}\sum_{k=1}^{M}e^{j\pi\alpha(k)}(e^{-pT\varepsilon kA}-e^{-pT\varepsilon kB})\right] \quad (13)$$

Based on the relation between **V** (p) and $\mathbf{C}_k$

$$C_k = \left[\frac{1}{T_1}(1-e^{-pT_1})V(p)\right]_{p=jk\omega_1} \qquad (14)$$

we can derive the analytical form for the Fourier coefficients:

$$C_\nu = C_{1+6\nu} + C_{3+6\nu} = \frac{2V_{dc}e^{-j\pi/6}}{\sqrt{3}\pi j(1+6\nu)} \cdot \sum_{k=1}^{M} \exp(j\pi\alpha(k)/3)\left[\exp(-j(1+6\nu)\frac{\pi}{3}\varepsilon_{kA} - \exp(-j(1+6\nu)\frac{\pi}{3}\varepsilon_{kB}\right] + \frac{V_{dc}e^{j\pi/2}}{\sqrt{3}\pi j(3+6\nu)} \cdot \sum_{k=1}^{M} \exp(j\pi\alpha(k)\left[\exp(-j(3+6\nu)\frac{\pi}{3}\varepsilon_{kA} - \exp(-j(3+6\nu)\frac{\pi}{3}\varepsilon_{kB}\right] \qquad (15)$$

From (15) we can derive by the inverse the analytical equations for the Fourier series of the phase voltages as follows:

PHASE A:

$$u_A(n,\varepsilon) = \sum_{\nu=-\infty}^{\infty}\left[\frac{-4V_{dc}}{\pi\sqrt{3}(1+6\nu)}\sum_{k=1}^{M}\left[\sin\frac{\pi}{6}(1+6\upsilon)\Delta\varepsilon_k\right] \sin\left[(1+6\nu)\left[\omega_1(n+\varepsilon)T - \frac{\pi}{6}(\varepsilon_{kA}+\varepsilon_{kB})\right] + \frac{\pi\alpha(k)}{3} - 2\pi/3\right]\right] +$$

$$+ \sum_{\nu=-\infty}^{\infty}\left[\frac{-2V_{dc}}{\pi\sqrt{3}(3+6\nu)}\sum_{k=1}^{M}\left[\sin\frac{\pi}{6}(3+6\upsilon)\Delta\varepsilon_k\right] \sin\left[(3+6\nu)\left[\omega_1(n+\varepsilon)T - \frac{\pi}{6}(\varepsilon_{kA}+\varepsilon_{kB})\right] + \pi\alpha(k)\right]\right] \qquad (16)$$

Similarly, we obtain for the next phases:

PHASE B and C:

$$u_B(n,\varepsilon) = \sum_{\nu=-\infty}^{\infty}\left[\frac{-4V_{dc}}{\pi\sqrt{3}(1+6\nu)}\sum_{k=1}^{M}\left[\sin\frac{\pi}{6}(1+6\upsilon)\Delta\varepsilon_k\right] \sin\left[(1+6\nu)\left[\omega_1(n+\varepsilon)T - \frac{\pi}{6}(\varepsilon_{kA}+\varepsilon_{kB})\right] + \frac{\pi\alpha(k)}{3}\right]\right] +$$

$$\sum_{\nu=-\infty}^{\infty}\left[\frac{-2V_{dc}}{\pi\sqrt{3}(3+6\nu)}\sum_{k=1}^{M}\left[\sin\frac{\pi}{6}(3+6\upsilon)\Delta\varepsilon_k\right] \sin\left[(3+6\nu)\left[\omega_1(n+\varepsilon)T - \frac{\pi}{6}(\varepsilon_{kA}+\varepsilon_{kB})\right] + \pi\alpha(k) + 2\pi/3\right]\right] \qquad (17)$$

From (16) and (17) it may be seen that the fundamental harmonic is lowered by $\sqrt{3}$,as compared with the fundamental harmonic in the classical B6 inverter.

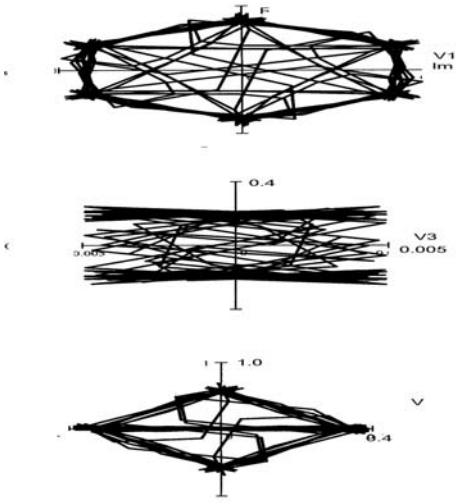

Fig.-3 Fourier aproximation of voltage space vectors. Top: first symmetrical sequence. Middle : second symmetrical sequence. Bottom : Overall sequence.

It may be also proved for the voltage in phase A that the second term in (16) is always zero. This is given by the fact that for each harmonic with order k=3+6ν, there arise two parts with the same amplitudes but with the opposite sign which cancel each other.

The derived analytical equations were visualized for the graphical form by the programme MATCAD and some results of the frequency-domain analysis are shown in Fig.3

In Fig.3 we can see the Fourier series of the first symmetrical component of the voltage space-

vectors $\mathbf{V}_1$ (top), the Fourier series of the second symmetrical component $\mathbf{V}_3$ (middle) and the Fourier series for the overall voltage space vector $\mathbf{V}$ (bottom). The parameters of modulation are N_1=4, g=1 and f1=50 Hz.

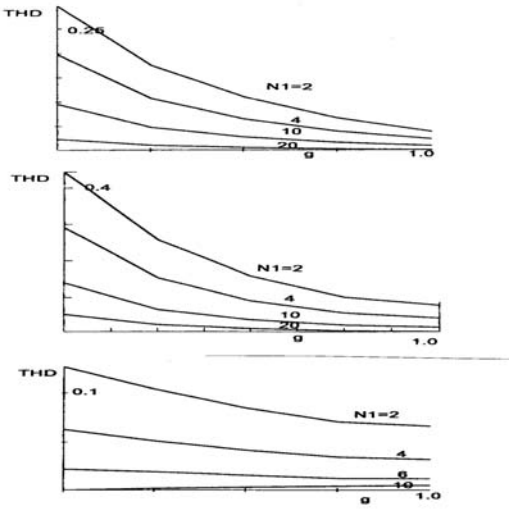

Fig.-4. Total harmonic distortion (THD) versus modulation factor g. (Top)-phase A,post-fault regime. (Middle)-phase B and C post-fault regime.
(Bottom)-pre-fault regime

The calculations were performed for the harmonics $-40 \le \nu \le 40$.
As it was mentioned earlier, in the phases B and C the harmonic spectrum also contains the third order harmonics given by second term in (17).
Fig.4 shows dependency of total harmonic distortion (THD) versus modulation factor g, for different values of sampling frequency given by the factor N_1 in the phase A and B, respectively. From Fig.4 we can see that the harmonic content in the B4 inverter and phase connected with the centre point of the DC supply is for the values $g \ge 0.5$ similar to the B6 inverter.THD in the both phase B and C contains also the third order harmonics and is higher than THD in phase A.
The higher values can again be obtained in the overmodulation region up to six-step regime.
In six-step regime THD for the phase A is the same as in the B6 inverter THD=0.0461.In the both remaining phases is THD owing to the third order harmonics higher and it has value: THD=0.201

4 Experimental verification

A 4-kVA prototype was constructed using 400V, 30A IGBT module, and two 2000μF capacitors.

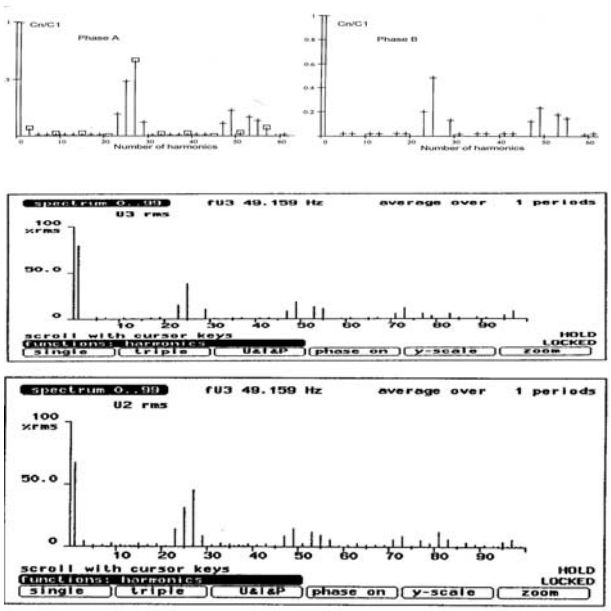

Fig.-5. Voltage harmonic spectrum .Analytical calculated (top trace).Experimental measured (middle trace)phase A ,(bottom trace) phase B and C.

A 2, 7 kW, 4-pole, 400/230V, 50 Hz, induction motor was used as a load of the inverter. The output inverter was operated with the suggested space-vector PWM .Texas Instruments TMS320F2407 DSP processor was used for the control of the system.
The measured voltage spectra in phase A and phase B are shown in Figs.5 ,respectively to compare the proposed space vector modulation analytical spectrum, given by (16) and (17) Fig.5 shows the measured harmonic spectrum in the phase A for the parameters
(N_1=4,f_{SW}=1200Hz, f_1=50Hz, g=1.0).From the top of the figure we can also see the theoretical spectra given by (16) and (17). As we can see there is an excellent agreement between the analytically calculated waveforms and the experimentally determined ones. As it was explained earlier the voltage spectra is different for the phase connected with centre tap of the DC supply., and for the two remaining phases. The difference is given by the third order harmonics in phases not connecting with centre tap of the DC supply. (These harmonics are depicted in Fig.5 by boxes)

5 Conclusion

The paper has presented an extension of the decomposition technique for the frequency-analysis of the synchronous space-vector modulation strategy both in the (B6) and (B4) inverters. The proposed modulation strategy aims minimizing voltage alternating sequence that originates third order harmonics in the both phases not connecting with the centre-point of the DC supply. As shown, there is an excellent agreement between the analytical calculated harmonic spectra and the experimentally determined ones. Measured and analytically calculated waveforms indicate small low-order harmonics and thus, an acceptable performance of the proposed modulation strategy.

REFERENCES

[1] H.Broeck, H.C. Skudelny, " *Analytical analysis of the harmonic effects of a PWM ac drive."*.IEEE Trans.Power Electron.vol.3,pp.216-222,1988.

[2] H.Broeck,J.D. Van Wyk, " *A comparative investigation of a three-phase induction machine drive with a component minimised voltage-fed Inverter under different control options*.". IEEETrans.Ind.Appl.. vol. IA-20,pp.309-320.,1984

[3] F.Blaabjerg, S.,Freysson, H.,Hansen , S.,Hansen, " *A new optimised space-vector modulation strategy for a component -minimised voltage source inverter*." IEEE Trans.Power Electron.vol.12,,pp.704-713,1997

[4] D.Kastha,B.K.Bose.: "*Investigation of fault modes of voltage-fed inverter system for induction motor drive"*.IEEE Trans.Ind.Appl.,vol.30,pp.259-266,1994

[5] D.Kastha,B.K.Bose.:"*Fault mode single phase operation of a variable frequency induction motor drive and improvement of pulsating torque characteristic*."IEEE Trans.Ind.Electron.vol.41,pp.426-433,1994

[6] G.T. Kim , A.T. Lipo,"*VSI-PWM rectifier-inverter system with a reduced switch counts*." IEEE Trans.Ind.Appl.vol.IA-32,,pp.1331-1337,1996.

[7] G.I. Peters,G.A.Covic , J.T.Boys," *Eliminating output distortion in four-switch inverters with three-phase loads."* IEE Proc.Electr.Power Appl..vol.IA-34, pp.326-332,1998.

[8] J,Klima," *Using of discrete Fourier transform for the analysis of the circuits with the periodical modulation.* "Journal of Electrical Engineering, vol.39,.,pp.257-265.,1988.

[9] J, Klima," *Mixed p-z approach for analytical analysis of an induction motor fed from space-vector PWM voltage source inverter* ".European Transaction on Electric Power.(ETEP), vol.12.No.6,pp.403-415,2002

[10] J.Klima," *Analytical investigation of an induction motor fed from B4 inverter with a new space-vector modulation strategy*."Proceedings of IEEE-IEMDC Conference,Madison,pp.1916-1923,2003

[11] P.Enjeti, A.Rahman*," A new single-phase to three-phase converter with active input current sharing for low cost ac motor drives*.."Proc.IEEE IAS 90,pp.935-939,1990.

[12] V. Sleger,P.Vrecion," *Matcad 7.*Haar International,Prague,1998

Proceedings of the 5th WSEAS Int. Conf. on Power Systems and Electromagnetic Compatibility, Corfu, Greece, August 23-25, 2005 (pp149-155)